

Letters

Quasi-Resonant Boost-Half-Bridge Converter With Reduced Turn-Off Switching Losses for 16 V Fuel Cell Application

Chansoo Park and Sewan Choi, *Senior Member, IEEE*

Abstract—An active-clamped current-fed converter can achieve not only lossless clamping but also zero-voltage switching. In particular, a boost-half-bridge (BHB) converter is one of the most suitable candidates for high-current, high-step-up applications owing to its low transformer turn ratio, reduced voltage rating of diodes, zero magnetizing dc offset, and symmetrical structure for all components. In this letter a quasi-resonant switching technique for a BHB converter with active clamping is proposed to significantly reduce turn-off switching losses. Experimental results for a 16 V, 1.2 kW prototype validate the effectiveness of the proposed concept.

Index Terms—Boost half bridge, current fed, fuel cell, quasi-resonant.

I. INTRODUCTION

SOLATED boost dc–dc converters are seeing increasing demand in many applications such as fuel cell systems, photovoltaic systems, hybrid electric vehicles, and uninterrupted power supply systems. Owing to the smaller input current ripple, lower diode voltage rating, and lower transformer turns ratio, the current-fed converter is better suited to high-step-up applications. Active-clamped current-fed converters have been developed with three different topologies: push pull [1], full bridge [2], [3], half-bridge [4]–[6]. They achieve not only lossless clamping of voltage spikes caused by transformer leakage inductance but also zero-voltage-switching (ZVS) of switches. The active-clamped push–pull converter has the simplest structure; however, center-tapping of the transformer on the low-voltage, high-current side could be a challenge in manufacturing. The active-clamped full-bridge converter requires an additional switch for clamping, and the switching frequency of the clamp switch should be twice that of the main switch. The active-clamped half-bridge converter in [4]–[6] does not have the aforementioned problems of the push–pull and full-bridge versions of

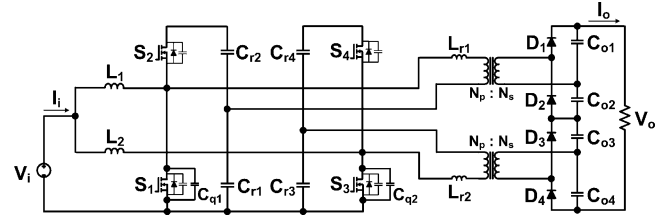


Fig. 1. Proposed quasi-resonant boost-half-bridge converter.

the active clamped converter. However, the active-clamped ZVS PWM converter in [4] may have the reverse-recovery problem of the output rectifying diodes [5]. The lower switches of the active-clamped converter with input-current doubler and output-voltage doubler in [5] are turned ON with hard switching and have high current stress. The active-clamped boost half-bridge (BHB) converter in [6] overcomes the drawbacks of the converters in [4], [5] and has the following advantages: no dc offset in magnetizing current; negligible current imbalance between each phases; ZVS turn-on of all switches; and a reduced voltage rating for rectifying diodes, allowing the use of inexpensive Schottky diodes. However, a major disadvantage is high turn-off current of switches.

In this letter, a quasi-resonant (QR) BHB converter is proposed to reduce the turn-off current by introducing resonant operation during switch turn-on process. The turn-off switching loss is further reduced by a small external capacitor across lower switches. This letter details the operating principle of the proposed method and presents experimental results for a 16 V, 1.2 kW prototype for validation.

II. PROPOSED CONVERTER

A. Operating principle

The circuit topology of the proposed converter is shown in Fig. 1. The use of separate clamp capacitors for each phase helps mitigate, without the need for current sensors, the current imbalance problem caused by volt-second imbalance between the two inductors. Furthermore, owing to the capacitor connection at both sides of the transformer, there must be no dc offset in the magnetizing current. In the proposed converter, capacitors $C_{r1} - C_{r4}$ are used to not only limit transient-surge voltage caused by transformer leakage inductance, but also resonate with the resonant inductors L_{r1} and L_{r2} during switch turn-on process so as to reduce turn-off current. The resonant frequencies of the tanks $L_{r1} - C_{r1}$ and $L_{r1} - C_{r2}$ are defined,

Manuscript received January 13, 2012; revised June 15, 2012 and October 4, 2012; accepted January 15, 2013. Date of current version May 3, 2013. This work was supported by the National Research Foundation of Korea grant funded by the Korea government under Grant 2012-0005045. Recommended for publication by Associate Editor R. Ayyanar

C. Park is with the AE Division, LG Electronics, Changwon 641-713, Korea (e-mail: chansoo1103.park@lge.com).

S. Choi is with the Department of Electrical and Information Engineering., Seoul National University of Science and Technology, Seoul 139-743, Korea (e-mail: schoi@seoultech.ac.kr).

Color versions of one or more of the figures in this paper are available online at <http://ieeexplore.ieee.org>.

Digital Object Identifier 10.1109/TPEL.2013.2243168

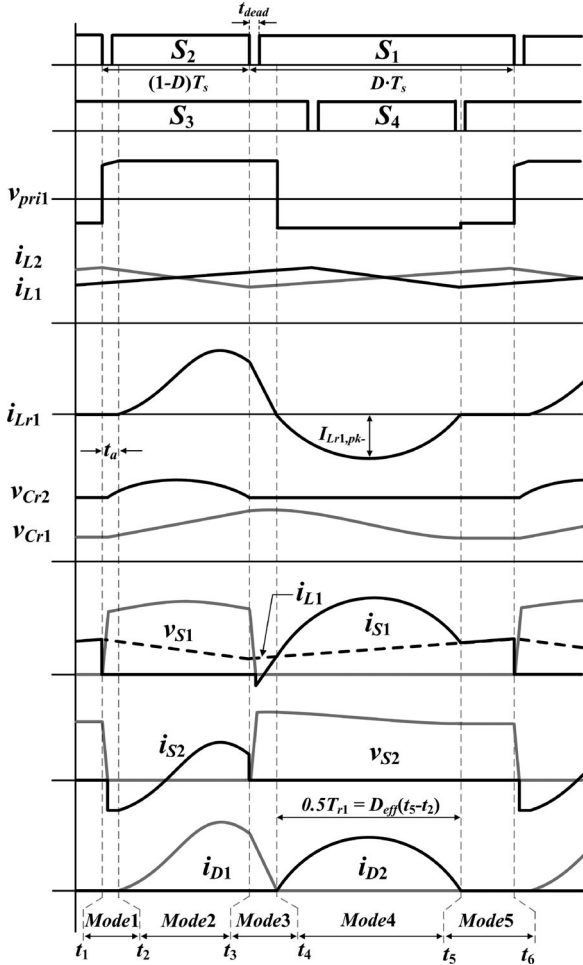


Fig. 2. Key waveforms of the proposed converter.

respectively, by

$$f_{r1} = \frac{1}{T_{r1}} = \frac{\omega_{r1}}{2\pi} = \frac{1}{2\pi\sqrt{L_{r1} \cdot C_{r1}}} \quad (1)$$

$$f_{r2} = \frac{1}{T_{r2}} = \frac{\omega_{r2}}{2\pi} = \frac{1}{2\pi\sqrt{L_{r1} \cdot C_{r2}}}. \quad (2)$$

Fig. 2 shows key waveforms of the proposed converter to illustrate the operating principle. The two legs are interleaved with a 180° phase shift, and the upper and lower switches of each leg are operated with asymmetrical complementary switching to regulate the output voltage. Fig. 3 shows equivalent circuits for the five operating modes.

Mode 1 starts at the moment S_1 is turned OFF and ends at the moment capacitor voltage reflected in the secondary, $n \cdot v_{Cr2}$, becomes greater than capacitor voltage v_{Co1} . The duration of Mode 1, $t_a = t_2 - t_1$, can be obtained by solving the following equation:

$$\frac{(C_{r1}/C_{r2})}{\omega_{r2} \cdot C_{r2}} \cdot \sin(\omega_{r2}(1-D)T_s - t_a) + t_a = 0. \quad (3)$$

In the proposed converter capacitor C_{r2} resonates with inductor L_{r1} during Mode 2, whereas capacitor C_{r1} resonates with inductor L_{r1} during Mode 4. Fig. 4(a) and (b) shows equivalent resonant circuits of Mode 2 and Mode 4, respectively. The

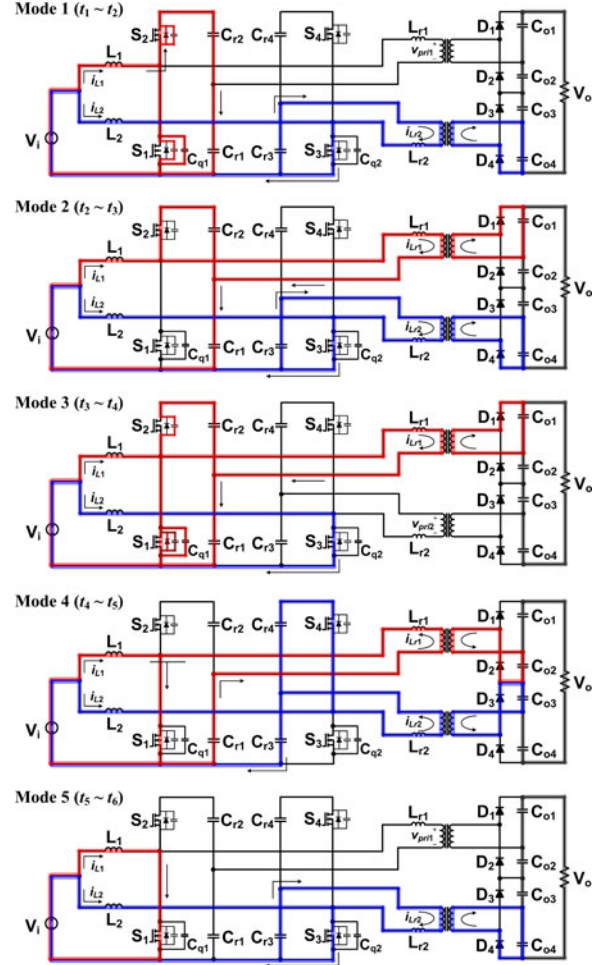


Fig. 3. Operation states of the proposed converter.

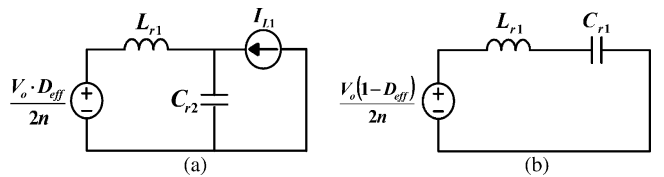


Fig. 4. Equivalent resonant circuits: (a) Mode 2 and (b) Mode 4.

resonant inductor currents during these modes are determined, respectively, as follows:

$$i_{Lr1}(t) = I_{L1} (1 - \cos \omega_{r2} \cdot t) \quad (\text{Mode 2}) \quad (4)$$

$$i_{Lr1}(t) = I_{Lr1,pk-} \sin(\omega_{r1} \cdot t) \quad (\text{Mode 4}) \quad (5)$$

where I_{L1} is the average value of the inductor current, and the peak value of the resonant current $I_{Lr1,pk-}$ can be obtained by

$$I_{Lr1,pk-} = \frac{n \cdot I_o}{2C_r \cdot f_s} \sqrt{\frac{C_{r1}}{L_{r1}}} \quad (0.5 \cdot T_{r1} \leq D \cdot T_s) \quad (6)$$

$$I_{Lr1,pk-} = \frac{n \cdot I_o}{C_{r1} \cdot f_s \cdot \cos(D \cdot T_s \cdot \omega_{r1})} \sqrt{\frac{C_{r1}}{L_{r1}}} \quad (0.5 \cdot T_{r1} > D \cdot T_s). \quad (7)$$

As a result of these resonant operations, turn-off currents of S_1 and S_2 become smaller than those of the PWM scheme [6], as

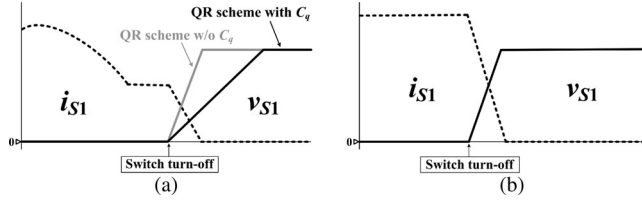


Fig. 5. Turn-off waveforms of the lower switch: (a) QR scheme and (b) PWM scheme.

shown in Fig. 2. Even if turn-off switching losses are reduced due to the proposed resonant operation, the switches are still turned OFF with hard switching. Adding external capacitor C_{q1} across lower switch S_1 makes switch voltage v_{S1} increase linearly with a slope of $i_{L1}(t_1)/(C_{q1} + 2C_{\text{oss}})$, resulting in near ZVS turn off. The same is true for S_2 . Fig. 5 shows turn-off waveforms of lower switch of the proposed QR scheme and PWM scheme in [6]. The QR scheme with C_q has the smallest turn-off switching losses while the PWM scheme has very large turn-off losses. However, increased equivalent output capacitance of a lower switch may cause a failure in ZVS turn-on of the switch. In order to ensure ZVS turn-on of lower switches at full load C_{q1} ($=C_{q2}$) are limited using the following equation:

$$C_{q1} \leq \frac{t_{\text{dead}} (i_{Lr1}(t_3) - i_{L1}(t_3)) (1 - D)}{V_{\text{in}}} - 2C_{\text{oss}}. \quad (8)$$

Furthermore, S_1 and S_2 are turned ON with ZVS because C_{r1} and C_{r2} are operated as not only resonant capacitors but also clamp capacitors of the active-clamp circuit. Also, it is noted that diode D_2 is turned OFF with ZCS owing to the resonant operation. Diode D_1 could be turned OFF with ZCS if L_{r1} is moderately large since i_{D1} decreases linearly with a slope of $(v_{Cr1} + (V_o \cdot D_{\text{eff}}/2n))/L_{r1}$.

B. Design Methodology

In this section, a design example is provided to determine the optimal resonant frequencies of the resonant tanks $L_{r1} - C_{r1}$ and $L_{r1} - C_{r2}$. The example specifications are as follows: $P_o = 1140$ W; $V_i = 12.8\text{--}26$ V (nominal input : 16 V); $V_o = 360$ V; $D = 0.29\text{--}0.69$ (nominal duty D_{nom} : 0.6); $f_s = 30$ kHz; $\Delta I_i = 3\%$; $\Delta V_o = 2\%$.

Fig. 6 shows the switch current waveforms corresponding to different resonant periods T_{r1} and T_{r2} in order to illustrate three operations; QR operation, boundary operation, and PWM operation. In cases (i) and (ii), the turn-off current for S_1 is the same; however, it is larger for (iii). Similarly, in cases (iv) and (v), the turn-off current for S_2 is zero; however, in case (vi), there exists large turn-off current. Large turn-off current may cause voltage spikes across the switch as well as large turn-off switching losses. The RMS and turn-off currents of the switches are plotted as functions of resonant frequency in Fig. 7. Therefore, resonant frequencies should be designed considering this boundary condition. In this example the optimal resonant frequency for lower switch is 27 kHz and is determined by

$$f_{r1} = \frac{f_s}{2D_{\text{nom}}}. \quad (9)$$

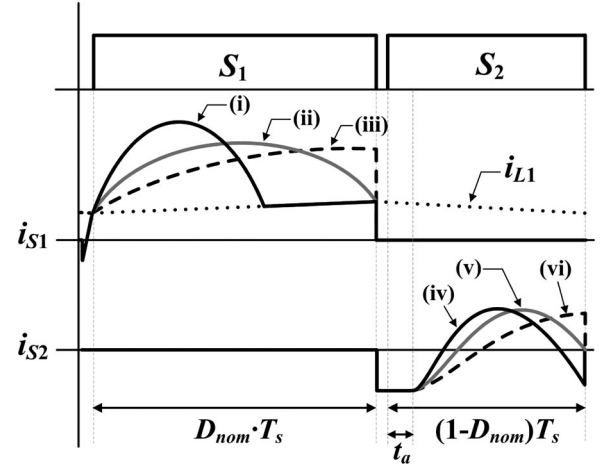


Fig. 6. Switch current waveforms corresponding to different resonant periods T_{r1} and T_{r2} : (i) QR operation ($0.5T_{r1} < D \cdot T_s$), (ii) Boundary operation ($0.5T_{r1} = D \cdot T_s$), (iii) PWM operation ($0.5T_{r1} > D \cdot T_s$) [6], (iv) operation ($0.75T_{r2} < (1-D)T_s - t_a$), (v) Boundary operation ($0.75T_{r2} = (1-D)T_s - t_a$), and (vi) PWM operation ($0.75T_{r2} > (1-D)T_s - t_a$) [6].

Also, using (1) and (9), resonant capacitance C_{r1} ($=C_{r3}$) can be obtained by

$$C_{r1} = \frac{1}{L_{r1}} \left(\frac{D_{\text{nom}}}{\pi f_s} \right)^2. \quad (10)$$

Similarly, the optimal resonant frequency for the upper switch is 61 kHz and is determined by

$$f_{r2} = \frac{3}{4} \left(\frac{f_s}{1 - D_{\text{nom}} - f_s \cdot t_a} \right) \quad (11)$$

Also, using (1) and (11), resonant capacitance C_{r2} ($=C_{r4}$) can be obtained by

$$C_{r2} = \frac{2}{3\pi L_{r1}} (1 - D_{\text{nom}} - f_s t_a). \quad (12)$$

Now, some remarks are made to clarify the difference in resonant operation and its effect on performance between the proposed converter and the converter in [5].

The converter in [5] has one resonant tank whose resonant period is designed to be two times of $(1-D)T_s$, meaning that the resonant operation for both switches should be completed within $(1-D)T_s$. In the fuel cell application the highest duty cycle should be used at full-load condition. The shortened resonant period results in increased switch current stress. On the other hand, the proposed converter has two resonant tanks. The resonant period for the upper switch is designed to be $(1-D)T_s$ while the resonant period for the lower switch is designed to be DT_s . Therefore, the lower switch (main switch) has the longest resonant period at full load resulting in reduced switch peak current compared to the converter in [5]. Besides, all switches of the proposed converter are turned ON with ZVS whereas the lower switch of the converter [5] is turned ON with hard switching. The upper switch of the converter [5] is turned OFF with ZCS, but the reverse recovery problem associated with the MOSFET body diode exists. The comparison of main characteristics and

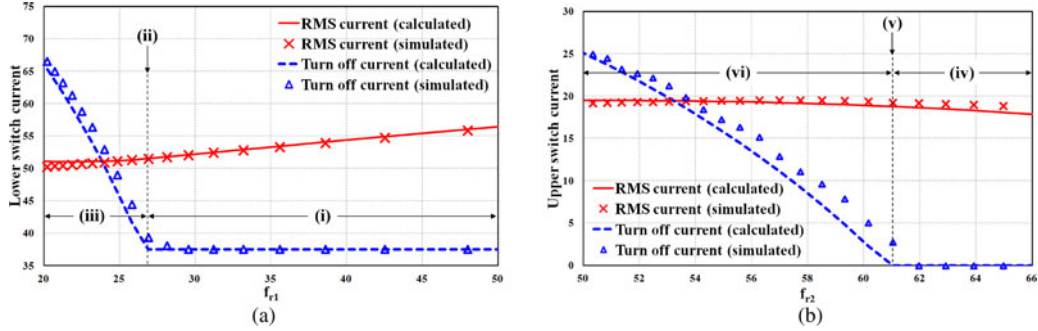


Fig. 7. RMS current and turn-off current as a function of resonant frequency: (a) lower switch and (b) upper switch.

TABLE I
COMPARISON OF THE PROPOSED AND CONVENTIONAL CONVERTERS ($P_o = 1140$ W, $V_i = 16$ V, $V_o = 360$ V, $f_s = 30$ kHz)

		Proposed Converter		Converter in [5]	
Switch waveforms		<p>Switch waveforms for the proposed converter. Top: Lower switch S_1 turns on at $v_{S1} = 0$ with ZVS, reaches a peak current $i_{S1,pk} = 81A$ at $t = DT_s$, and turns off at $v_{S1} = 0$ with ZVS. Bottom: Upper switch S_2 turns on at $v_{S2} = 0$ with ZVS, reaches a peak current $i_{S2,pk} = 9A$ at $t = (1-D)T_s$, and turns off at $v_{S2} = 0$ with ZVS.</p>	<p>Switch waveforms for the converter in [5]. Top: Lower switch S_1 turns on at $v_{S1} = 0$ with hard switching, reaches a peak current $i_{S1,pk} = 108A$ at $t = (1-D)T_s$, and turns off at $v_{S1} = 0$ with ZVS. Bottom: Upper switch S_2 turns on at $v_{S2} = 0$ with hard switching, reaches a peak current $i_{S2,pk} = 38A$ at $t = (1-D)T_s$, and turns off at $v_{S2} = 0$ with ZVS.</p>		
Switching method	S_1, S_3	ZVS turn-on Turn off current = 38A	Hard switched turn-on Turn off current = 38A		
	S_2, S_4	ZVS turn-on Turn off current = 9A	ZVS turn-on The reverse recovery problem of the body diode exists		
Diode rating		4 EA / 180 V, 3.1 A _{av}		2 EA / 360 V, 3.1 A _{av}	
Transformer	Turn ratio	1 : 5		1 : 5	
	VA rating	707 VA × 2		1475 VA	

device ratings of the proposed converter and the converter in [5] is summarized in Table I.

III. EXPERIMENTAL RESULTS

Two 1.2 kW laboratory prototypes of the proposed QR scheme and PWM scheme [6] are built with the specifications given in Section II-B. The prototype of the proposed converter is implemented under the following parameters and components— $S_1 - S_4$: IRFP4368 × 2; $D_1 - D_4$: MBR40250; L_1, L_2 : 60 μ H; L_{r1}, L_{r2} : 0.4 μ H; C_{r1}, C_{r3} : 90 μ F; C_{r2}, C_{r4} : 17 μ F; C_{q1}, C_{q2} : 52 nF; $C_{o1} - C_{o4}$: 15 μ F.

Each transformer is built using PQ40/40 core with the number of turns of $N_p:N_s = 5:25$. The leakage inductance of the transformer, which is measured as 0.4 μ H, is used as the resonant inductance L_{r1} ($=L_{r2}$).

Figs. 8 and 9 show the experimental waveforms of the proposed QR and PWM schemes, respectively, at 1140 W load. It

can be seen that all switches were turned ON with ZVS, and the turn-off currents with the proposed QR scheme were significantly reduced compared to those with the PWM scheme. The measured efficiencies of both the QR and the PWM schemes are shown in Fig. 10. The peak and full load efficiencies of the proposed QR scheme with C_q were 96.3% at 310 W and 93.7% at 1140 W, respectively.

Fig. 11 shows calculated switch losses of the PWM scheme and QR scheme at full and light loads. At full load, ZVS turn-on is achieved for all three schemes. The QR scheme with C_q has the smallest turn-off losses owing to the proposed resonant operation and external capacitors across lower switches. At light load, the switches of the QR scheme with C_q are turned ON with hard switching, resulting in poor light load efficiency. Nevertheless, since the QR scheme with C_q has the highest full load efficiency it is the most suitable for fuel cell applications, where the system is operated at full load during most of the time.

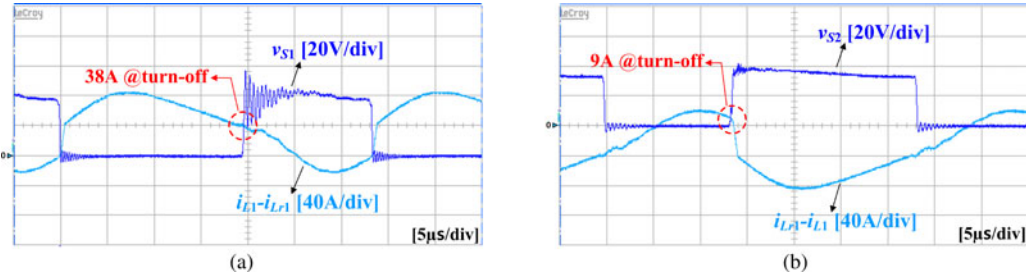


Fig. 8. Experimental waveforms for the proposed QR scheme with C_q : (a) lower switch and (b) upper switch.

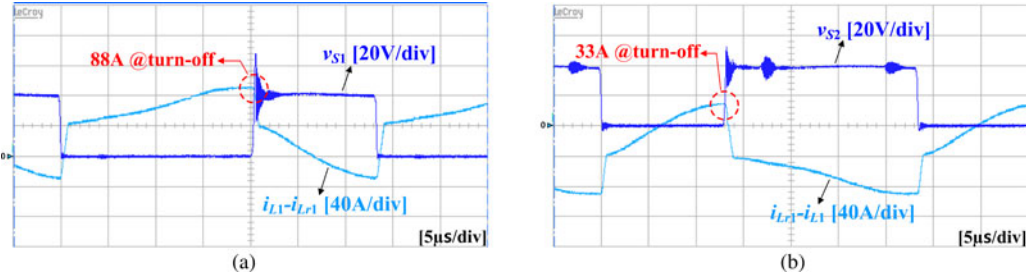


Fig. 9. Experimental waveforms for the PWM scheme [6]: (a) lower switch and (b) upper switch.

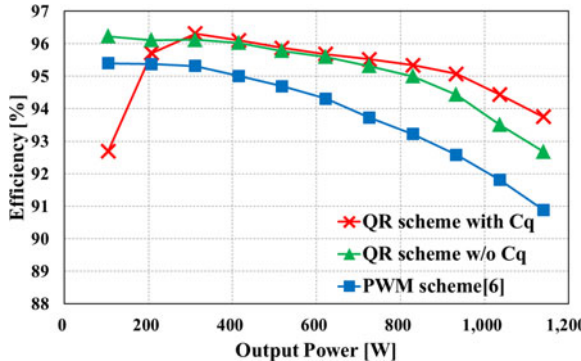


Fig. 10. Measured efficiencies of the QR and PWM schemes.

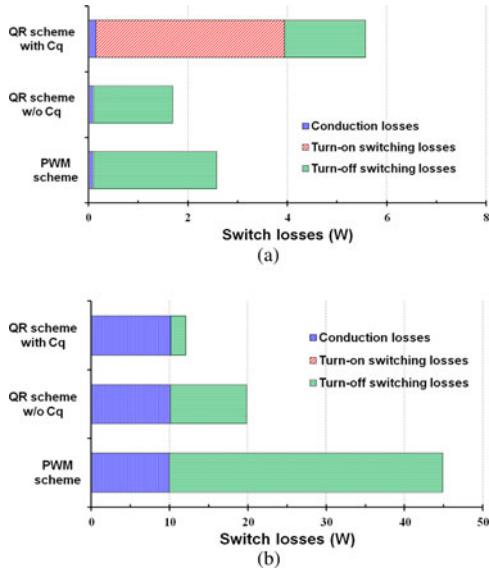


Fig. 11. Switch loss comparison of the QR and PWM schemes: (a) at light load ($P_o = 100$ W) and (b) at full load ($P_o = 1140$ W).

IV. CONCLUSION

This letter proposed an improved switching method for an active-clamped BHB converter for high-step-up applications. The proposed circuit structure helps mitigate, without the need for current sensors, the current imbalance problem and eliminate dc offset in the magnetizing current. The proposed converter achieves ZVS turn ON of switches and ZCS turn OFF of diodes. The turn OFF current of switches is significantly reduced by introducing the proposed resonant operation. Adding external capacitors across lower switches results in near ZVS turn OFF of switches. Experimental results from 1.2 kW prototypes validated that the proposed QR scheme has 2.8% better full-load efficiency compared to the PWM scheme, meaning that the QR scheme is better suited to fuel cell applications.

REFERENCES

- [1] F. J. Nome and I. Barbi, "A ZVS clamping mode-current-fed push-pull DC-DC converter," in *Proc. IEEE Int. Symp. Ind. Electron.*, 1998, vol. 2, pp. 617–621.
- [2] V. Yakushev, V. Meleshin, and S. Fraidlin, "Full-bridge isolated current fed converter with active clamp," in *Proc. IEEE App. Power Electron. Conf. Expo*, 1999, vol. 1, pp. 560–566.
- [3] R. Watson and F. C. Lee, "A soft-switched, full-bridge boost converter employing an active clamp circuit," in *Proc. IEEE Conf. Power Electron. Spec. Conf. Rec.*, 1996, vol. 2, pp. 1948–1954.
- [4] S. Han, H. Yoon, G. Moon, M. Youn, Y. Kim, and K. Lee, "A new active clamping zero-voltage switching PWM current-fed half-bridge converter," *IEEE Trans. Power Electron.*, vol. 20, no. 6, pp. 1271–1279, Nov. 2005.
- [5] J. Kwon and B. Kwon, "High step-up active-clamp converter with input-current doubler and output-voltage doubler for fuel cell power systems," *IEEE Trans. Power Electron.*, vol. 1, no. 1, pp. 108–115, Jan. 2009.
- [6] H. Kim, C. Yoon, and S. Choi, "An improved current-fed ZVS isolated boost converter for fuel cell application," *IEEE Trans. Power Electron.*, vol. 25, no. 9, pp. 2357–2364, Sep. 2010.
- [7] P. Enjeti, "Power conditioning systems for fuel cell systems," in *Fuel Cell Handbook*, 6th ed. Washington, DC, USA: U.S. Department of Energy, 2002.